A MODEL OF KNOT SHAPE AND VOLUME IN LOBLOLLY PINE TREES

*Guillermo Trincado**

Assistant Professor
Instituto de Manejo Forestal
Universidad Austral de Chile
Box 567
Valdivia, Chile

Harold E. Burkhart

University Distinguished Professor
Department of Forestry
Virginia Polytechnic Institute and State University
Blacksburg, VA 24061

(Received December 2007)

Abstract. The shape and structure of branches attached internally to the stem (knots) for loblolly pine (*Pinus taeda* L.) trees were modeled. Data on knot shape were obtained from the dissection of branches taken from 34 22-yr-old sample trees growing under ten different initial spacings. A total of 341 branches located below the live crown were dissected in the radial/tangential plane. Afterward, a procedure was implemented to reconstruct the branch diameter perpendicular to the branch pith. This information was used to develop a model for representing knot shape, which assumed that the live portion of a knot can be modeled with a one-parameter equation and the dead portion by assuming a cylindrical shape. To study the variability in shape of individual knots (live portion), the model was fitted to 218 branch profiles using nonlinear mixed-effects modeling techniques. A graphical analysis indicated that the random-effects parameter was related to branch diameter. Thus, branch diameter was included as a predictor variable to reduce between-individual variability in knot shape. Reconstructed knots with smaller diameters were more cylindrical; those with larger diameters were more parabolic or conical in shape. Analytical expressions were derived for estimating the volume of knots (live/dead portions) for three types of branch conditions on simulated trees: 1) live branches; 2) nonoccluded dead branches; and 3) occluded dead branches. The knot model assumes a substantial simplification of branch morphology, but should be useful for representing knots as 3-D entities in the stems of loblolly pine trees.

Keywords: Wood quality, knot shape, knot volume, *Pinus taeda.*

INTRODUCTION

A knot represents the internal attachment of first-order branches to the tree stem (Lemieux et al 2001). Knot frequency, size, and location along and around the stem are determined by both the crown and branch dynamics. Silvicultural decisions such as initial planting density and spacing (Clark et al 1994; Sharma et al 2002; Amateis et al 2004), thinning (Baldwin et al 2000), pruning (Clark et al 2004), and fertilization (Yu et al 2003) have important effects on the size of branches and thus on knot dimensions. Clark and McAlister (1998) developed a new tree grading system for southern pines based on the number and size of branches in the lower part of the bole. They found that the inclusion of branch variables improved the prediction in expected lumber grade yield. Furthermore, size and location of knots are important characteristics for determining grade of solid wood products such as dimension lumber (Haygreen and Bowyer 1996).

* Corresponding author: gtrincad@uach.cl

From a wood quality perspective, knots are considered defects that reduce the value of the raw material, because they decrease the strength and stiffness of wood intended for structural uses (Whiteside et al 1977; Briggs 1996; Gartner 2005). Their effect on mechanical properties is the result of the interruption of continuity and change in the direction of wood fibers (Grace et al 1999). Despite their importance in determining wood quality, first-order branch development and knots have not been thoroughly studied in loblolly pine (*Pinus taeda* L.). The study of branch development and knot formation can permit construction of predictive models for these variables and enhance the capability of individual tree growth and yield simulation systems.

In a simulation framework, knots need to be represented as 3-D entities. Generally, external information of branches, such as diameter, azimuth, location in a log, and angle of inclination, are used to project knots internally assuming a certain geometric shape (eg, Barbour et al 2003). Sawing simulators such as SEESAW (García 1987) and SIMQUA (Leban and Duchanois 1990) represent the shape of knots contained in logs as cones. In contrast, in AUTOSAW, the live portion of a knot is represented with a cone, and the dead portion, attached to the end of the cone, is represented with a cylinder (Todoroki 1996). An analytical system of equations to describe the geometry of a large variety of knot shapes was reported by Samson et al (1996). However, despite the flexibility of this system, the complexity and amount of parameters (ie, 17 parameters) required to represent knots make the implementation of this model unfeasible for most practical applications. Lemieux et al (1997) reported on a reduced expression of this model that was used to smooth knot data for Norway spruce [*Picea abies* (L.) Karst].

The inclusion of knots in the simulation of tree stems requires a simpler representation of knots and the capability of maintaining spatial information (3-D) of their internal location along the stem. We present the development of a model for representing the internal knot shape and structure of loblolly pine trees. The specific objectives of this research were to 1) recover information on knot shape using a destructive analysis technique; 2) characterize the shape and structure (live/dead portion) of knots using a mathematical model; and 3) derive analytical expressions to predict the volume of individual knots from the derived model.

MATERIALS AND METHODS

Data

In 1983, spacing trials were established at four locations (two in the Atlantic Coastal Plain and two in the Piedmont) by using the experimental design of Lin and Morse (1975). The study consisted of three replications at each location. Each replication consisted of row and column spacing levels of 1.2, 1.8, 2.4, and 3.6 m, which resulted in 16 treatments with an equal number of trees per plot but different plot sizes and shapes (Sharma et al (2002) contains additional details about this tree spacing study).

Growing stock planted at each location was genetically improved 1–0 loblolly pine seedlings from a single nursery. During the first 3 yr after planting, both herbaceous and woody competing vegetation was controlled. From establishment to age 5, the diameter at groundline was measured annually. Beginning at age 5, the diameter at breast height (DBH) was measured annually. Through age 10, total tree height, height to live crown, and crown width were measured annually for all trees. Measures of crown width were carried out until age 12. Categorical tree condition of each individual tree was also recorded. After age 10, total tree height and height to live crown were measured biannually, whereas DBH and tree condition were measured annually.

Data for this research were obtained from the loblolly pine spacing study located near Appomattox, VA (Piedmont region). During the dormant season of 2004–2005, at stand age 22 yr old, 34 trees were selected for comprehensive measurements of whorl characteristics and sampling of whorl sections. Trees with a single stem

and no record of a visible broken top were selected. The main goal was to collect data to model the morphology of knots and the dynamics of first-order branches. Among the branch characteristics of interest were number of branches per whorl, branch orientation around the stem (azimuth), angle of insertion with respect to the stem pith (inclination), and diameter growth. Additional information on whorl number and location within growing seasons was available from field measurements and past measurements on crown recession. Trees were selected from ten different initial spacings.

Before each tree was felled, DBH outside bark at 1.37 m was measured using a caliper, and a vertical line on the within-row side of the stem was marked to an approximate height of 2 m. Once the tree was on the ground, this line was extended along the length of the stem. This line served as a reference (azimuth 0°) for determining the orientation of the sampled whorl sections. For each sample tree, the stump height (cm) and distance from stump height to tree tip (m) were measured. For each visible whorl, the following variables were measured: 1) height above ground (m); 2) diameter outside bark (cm); 3) status; and 4) number of visible branches or branch stubs in each whorl. The status of each whorl section was visually categorized as: live (all branches alive), sound (not all branches alive), or knot (no branches alive). After that, a number of whorl sections (3–5) located below the live crown were chosen randomly from each sample tree for subsequent laboratory dissection. Each whorl section was labeled for identification and marked on its bottom surface with the position of the reference line. A total of 217 whorl sections were collected in the field from the sample trees.

Dissection and Measurement of Knots

A dissection technique similar to that reported by Lemieux et al (2001) was used in this study to collect information on knot shape. Before dissection, each whorl was dried, debarked, and, when necessary, trimmed to fit on the band saw. After that, the sample whorl preparation procedure included: 1) identifying and labeling each visible branch proceeding clockwise from the reference line; 2) marking the largest branch and possibly a second branch on the opposite side of the stem; and 3) marking the top of the whorl section with the horizontal direction (azimuth) from the pith to bark of each branch identified in (1). From the 217 whorl sections, only 198 sections were suitable for dissection, because some sample sections could not be identified or were missing. Only one branch was selected from 42 whorl sections and two branches from 156 whorl sections for a total of 354 dissected knots. In addition, a disk was cut from the top and used to determine branch azimuth with a protractor and the width of each ring to the nearest 0.002 mm in the direction of branches selected for dissection. Ring width was measured using a tree ring measurement system (Velmex, Inc; Bloomfield, NY). Only 341 knots proved suitable for measurement of ring width, providing the final sample size for this study.

The sequence of cuts performed on each sample branch is presented in Fig 1. The distance between faces of consecutive slices from bark to pith was approximately 5 mm consisting of 3-mm samples and 2-mm kerf. In each slice, the distances from the bottom of the whorl section to the top, pith, and bottom of the knot were measured (vertical direction). Using the pith of the branch as a reference, another diameter measurement of the knot was made in the horizontal direction.

Reconstruction of Knot Profiles

The dissection procedure allowed measurement of knot diameters in the radial/tangential (R/T) plane from the stem pith. However, these measurements were not perpendicular to the main branch axis. A procedure was implemented to reconstruct the "true" branch diameters at a given branch age, which is defined as the branch diameter measured perpendicular to the branch axis. It was necessary to determine the number of years a branch was alive to identify the live

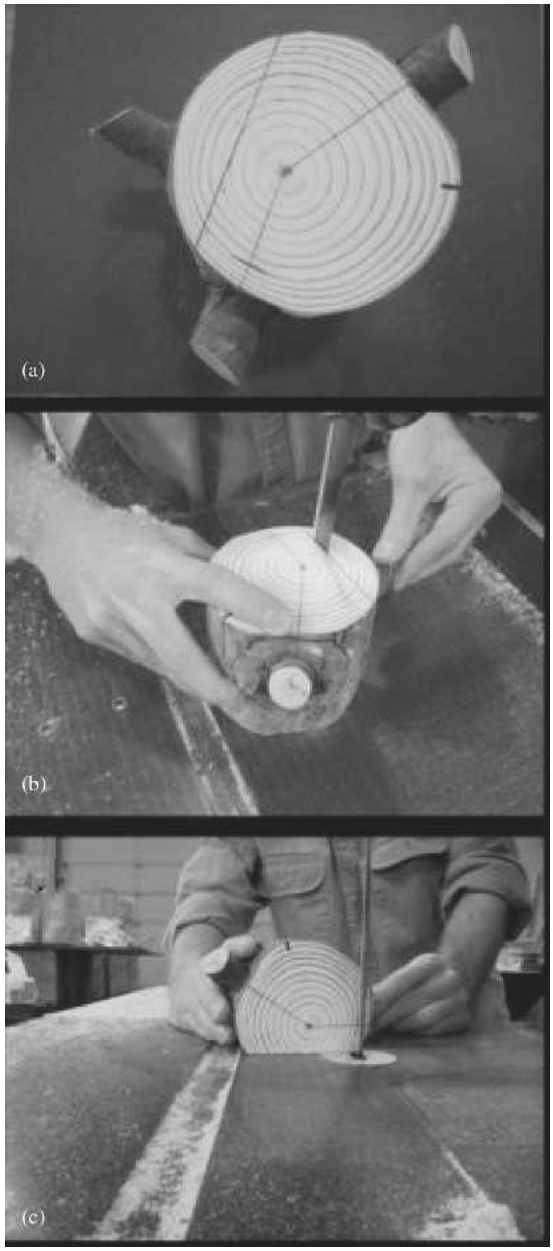

Figure 1. Procedure used for dissecting branches: (a) identification of target branches, (b) tangential cut for consistent positioning of the sample on the band saw, and (c) sawing branch into approximately 3-mm slices parallel to stem pith.

and dead portions later during the dissection of branches. The height of the whorl was used to determine the tree age when the whorl was created, and data on crown recession were used to estimate the number of years a branch was alive. This information was used in conjunction with the ring width measurements to estimate the stem diameters during the period in which a branch was alive. Given this information, the radial measurements of dissected branches (bark to pith) were referenced to actual stem radii. In Fig 2a, line B represents the radius of the stem and line A represents the radius of the stem at the estimated time of branch death. For this example, the branch was determined to be alive for a period of 10 yr given the crown recession data. Correspondingly, line A denotes the radial extent of the first 10 rings measured from the pith. The measurements taken on each knot were smoothed by fitting a growth curve to the diameter measurements and a linear regression curve to the branch pith (Fig 2b–c). The growth curve was a modified Weibull equation (Yang et al 1978):

$$y = \alpha\,(1 - \exp(-\beta\, x^{\gamma})) \qquad (1)$$

where y is the measured branch diameter parallel to the stem pith in mm; x is the knot length in mm; and α, β, and γ are estimated parameters. We assumed $\gamma = 1$ to reduce the number of estimated parameters (exponential equation).

To recover information on the live portion of a knot, the growth curve was fit only to points located to the left of line A (Fig 2b). Only branch samples with a minimum of five points to the left of line A were considered as adequate for this curve fitting and subsequent analyses. A total of 233 knot samples fulfilled this condition. Of the 233 samples, 15 did not converge when fitting the exponential function and were not used in subsequent analysis.

Fitting a linear regression equation to branch pith points provided information on the inclination angle of branches with respect to the stem pith (Fig 2c). Because this procedure assumed that the angle of inclination of branches is constant over time, a statistical analysis was applied to adequately test this observation. The statistical analysis involved fitting a quadratic model

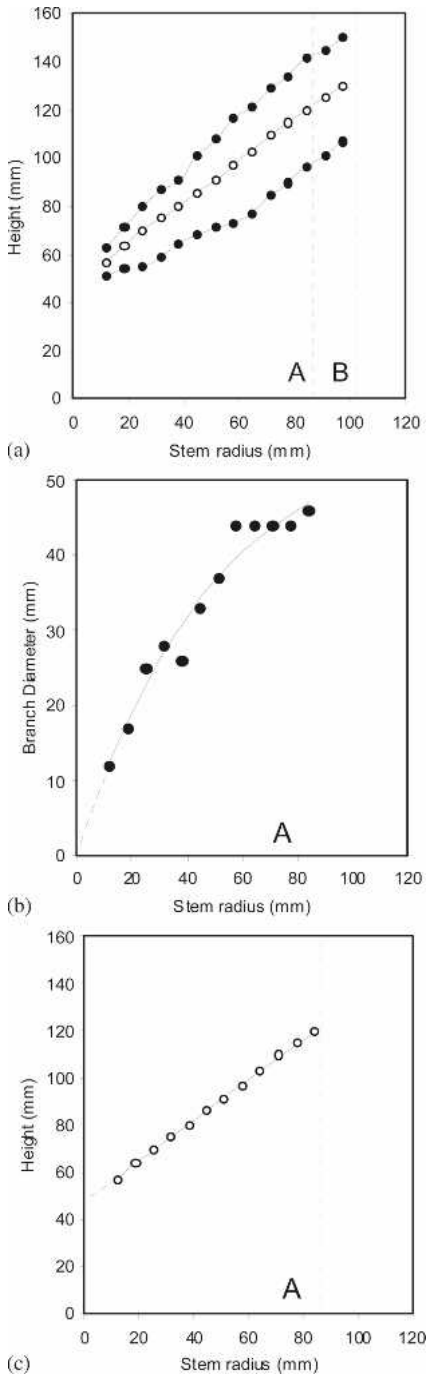

Figure 2. Measured (a) branch profile, (b) fitted growth curve to the diameter measurements, and (c) estimated linear regression through the branch pith.

and testing for the significance of the quadratic term.

The growth curve permitted interpolation of the branch diameters in the R/T plane (parallel to the stem pith) for each age (Fig 3a). The reconstruction permitted recovery of increases in diameter with branch age. However, it assumed that the branch pith passed through the center of the branch. Based on the smoothed branch profile and location of interpolated points, the true branch diameter for a given age perpendicular to branch pith was derived (Fig 3b). For each age, the calculation consisted of fixing the top point and passing a perpendicular line through the branch pith. Then, the intersection of this line with the bottom line of the smoothed branch profile defined the lower part of the branch for a given age. These reconstructed branch profiles were used later as basic information for modeling knot shape.

Model Development

Past research modeled knot geometry by projecting internal branches as cones (García 1987; Leban and Duchanois 1990) or assuming the live portion was a cone and the dead portion a cylinder (Todoroki 1996). Here, we considered that the live portion of a knot can be modeled with a simple mathematical equation and the dead portion by assuming a cylindrical shape. An additional assumption was that knots (not external branches) produced in fast-growing plantations have insignificant curvature, eg constant inclination from pith to bark. A simple equation to model the live portion of a knot is:

$$\frac{r_{(l)}^2}{R^2} = \kappa \left(\frac{l}{L}\right)^{\beta} \qquad 0 \le l \le L \qquad (2)$$

where $r_{(l)}$ is the radius (mm) of the live portion of a knot at length l (mm); R is the maximum radius (mm) of the live portion of a knot; L is the total length (mm) of the live portion of a knot; κ is the taper parameter; and β is the shape parameter. If $\beta = 1$, 2, or 3, the geometrical shape generated by Eq 2 is a paraboloid, cone, or

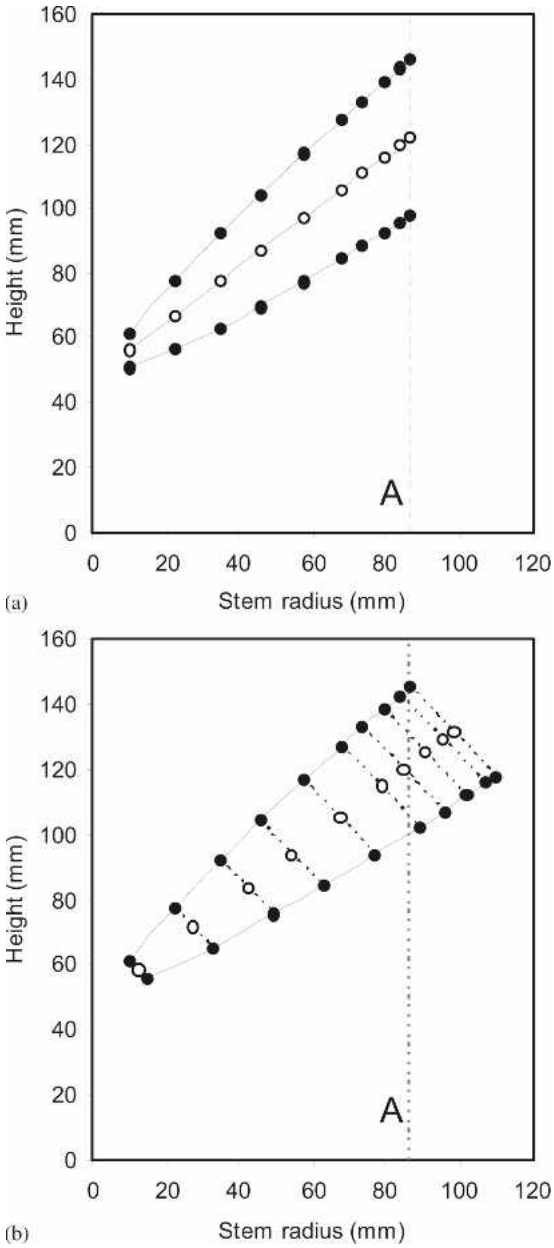

Figure 3. Smoothed (a) branch profile with interpolated branch diameters at a given branch age in the radial/tangential plane and (b) smoothed branch profile with branch diameters perpendicular to branch pith.

neiloid, respectively (Husch et al 2003). The model of the live portion of a knot meets two conditions: $r_{(l)} = 0$ when $l = 0$ and $r_{(l)} = R$ when $l = L$. The first condition is imposed by the model and the second condition can be met by making $\kappa = 1$. Therefore, the final model can be expressed as:

$$r_{(l)}^2 = R^2\left(\frac{l}{L}\right)^{\beta} \qquad 0 \le l \le L \tag{3}$$

Thus, knowing the total length of the live portion of a knot (L) and its maximum radius (R), it is possible to estimate the branch radius $r_{(l)}$ at any point inside the stem. Additionally, the volume of this portion of a knot can be estimated by applying integral calculus:

$$V = \pi R^2 \int_0^L \left(\frac{l}{L}\right)^{\beta} dl \tag{4}$$

It should be noted that the shape of the live part of a knot is determined by only one parameter (β), and the equation is highly tractable mathematically. A similar formulation (Eq 2) has been adopted when modeling stem form profiles (eg, Kozak 1988).

Volume Estimate for Branches Internally Attached to the Stem

A practical implementation of a knot model required derivation of a series of expressions to estimate the volume of branches attached internally to the stem (knots). The calculation of volume for the live and dead portions of any given knot was also considered. The following sections develop volume estimates for three types of branch conditions: 1) live branches; 2) nonoccluded dead branches; and 3) occluded dead branches (Fig 4).

Knot volume for a live branch. Determination of the spatial location of a live knot and its dimensions (diameter and length) required the coordinates of the branch origin O = (X_O, Y_O, Z_O), branch inclination (α, vertical angle in degrees with respect to stem pith), branch azimuth (θ, horizontal angle in degrees), branch diameter ($2R = |\overrightarrow{SP}|$, Fig 4a), and stem radius r at the point where the branch arises at the stem pith M = (X_M, Y_M, Z_M). Branches from the same whorl were assumed to have the same origin O. The

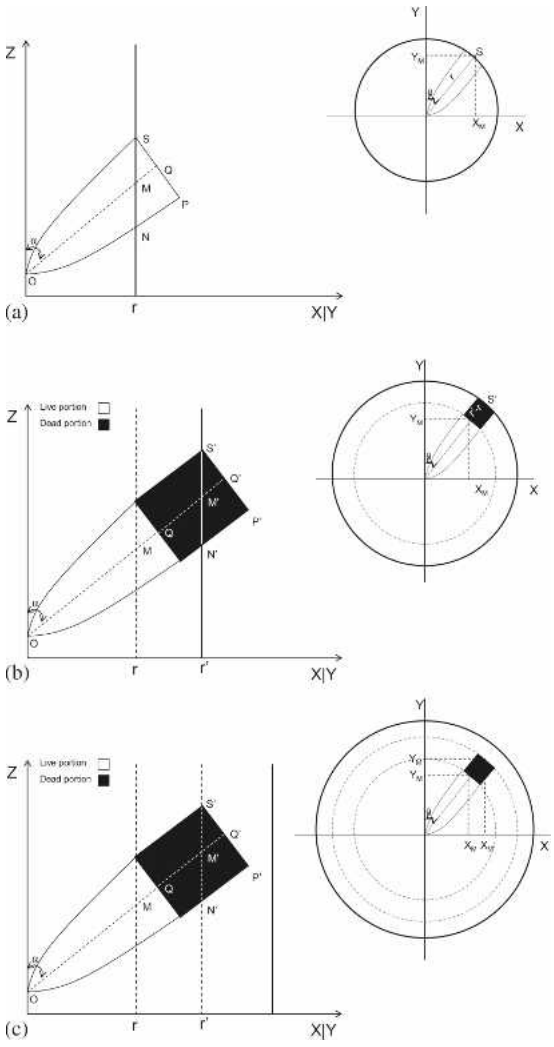

Figure 4. Type of branch conditions on simulated trees (a) live branch, (b) nonoccluded dead branch, and (c) occluded dead branch, where r and r' represent the stem radius at the height a branch arises from the stem bole.

origin was located in the center of the stem pith at a given height (Z_O) above the ground, so the values for X_O and Y_O were equal to zero, eg O = (0, 0, Z_O).

Internal knot length was the Euclidian distance $|\overrightarrow{OM}|$ between the point (0, 0, Z_O) and the point *M* where the branch arises at the stem pith (X_M, Y_M, Z_M). The coordinates for point *M* and subsequent knot length were calculated using the branch inclination (α), branch azimuth (θ), and the stem radius *r* at the height where a branch arises by using a taper equation. Thus, the coordinates where the branch pith arises from the stem were determined from the following relationships:

$$X_M = r \sin(\theta),$$
$$Y_M = r \cos(\theta),$$
$$Z_M = Z_O + r \tan(90\text{-}\alpha).$$

To facilitate calculations, it is recommended to use the same units (mm) in each of the three axes (X, Y, Z). Furthermore, to facilitate derivation of an approximation formula for the knot volume, the following variables were defined (see Fig 4a):

$$|\overrightarrow{OM}| = [X_M^2 + Y_M^2 + (Z_O - Z_M)^2]^{1/2},$$
$$|\overrightarrow{MQ}| = \frac{|\overrightarrow{SQ}|}{tg(\alpha)} = \frac{R}{tg(\alpha)},$$
$$L = |\overrightarrow{OQ}| = |\overrightarrow{OM}| + |\overrightarrow{MQ}|,$$
$$l = |\overrightarrow{NP}| \approx \frac{|\overrightarrow{SP}|}{tg(\alpha)} = \frac{2\,R}{tg(\alpha)}.$$

The approximate volume of the live branch contained in the internal part of the stem, referred to as the knot volume of the live portion (V_{LP}), was computed as:

$$V_{LP} = \pi R^2 \int_0^L \left(\frac{l}{L}\right)^{\beta} dl - V_L \qquad (5)$$

where an approximation for the volume of the limb (V_L) was obtained using the following formula:

$$V_L \approx \frac{\pi R^2 L}{2(\beta + 1)} [1 - ((L - l)/L)^{\beta+1}] \qquad (6)$$

Thus, the volume of the live portion (V_{LP}) of the knot was estimated using the following approximate formula:

$$V_{LP} \approx \frac{\pi R^2 L}{2(\beta + 1)} [1 + ((L - l)/L)^{\beta+1}] \quad (7)$$

For subsequent derivations of different branch conditions, the number of location points was expanded, but the definition of variables already used was maintained.

Knot volume for a nonoccluded dead branch. The geometrical representation of a live branch and the necessary location of points required to calculate its volume were presented in Fig 4b. The following additional variables were needed to characterize spatially a nonoccluded dead branch:

$$|\overrightarrow{OM'}| = [X_{M'}^2 + Y_{M'}^2 + (Z_O - Z_{M'})^2]^{1/2}$$

$$|\overrightarrow{M'Q'}| = \frac{|\overrightarrow{S'Q'}|}{tg(\alpha)} = \frac{R}{tg(\alpha)},$$

$$L' = |\overrightarrow{QQ'}| = |\overrightarrow{OQ'}| - |\overrightarrow{OQ}|$$
$$= |\overrightarrow{OM'}| + |\overrightarrow{M'Q'}| - |\overrightarrow{OQ}|,$$

$$l' = |\overrightarrow{N'P'}| \approx \frac{|\overrightarrow{S'P'}|}{\text{tg}(\alpha)} = \frac{2R}{\text{tg}(\alpha)}.$$

The volume of the live knot portion of a nonoccluded dead branch was obtained using Eq 4 as:

$$V_{LP} = \frac{\pi R^2 L}{(\beta + 1)} \quad (8)$$

and the volume for the dead portion of the knot (V_{DP}) was approximated with:

$$V_{DP} \approx \pi R^2 (L' - (l'/2)) \quad (9)$$

Furthermore, an expression for the total volume of the knot (V_T) was obtained by adding the volumes of live and dead portions:

$$V_T = \pi R^2 (L/(\beta + 1) + L' - (l'/2)) \quad (10)$$

Knot volume for an occluded dead branch. The volume for the live portion of an occluded branch (Fig 4c) was calculated using Eq 4 and the dead portion by applying the formula for a cylinder:

$$V_{DP} = \pi R^2 L' \quad (11)$$

Thus, the total volume of the knot was estimated using the following formula:

$$V_T = \pi R^2 (L/(\beta + 1) + L') \quad (12)$$

The proposed knot model allowed recovering efficiently the shape and volume of internal branches without increasing the amount of data generated for each branch during the simulation process. Only a dynamic update of the 3-D location of each point according to branch condition is required to make the necessary calculations (Fig 4).

Model Fitting and Validation

Knot profile data represent multiple observations from the same branch (see Fig 2c), violating the assumption of independent observations required in regression analysis (Judge et al 1985; Neter et al 1998). Under a well-specified model, the parameter estimates are still unbiased. However, the variance can be underestimated affecting confidence intervals and hypothesis testing (West et al 1984; Schabenberger and Pierce 2001). A more efficient method to obtain parameter estimates involves using nonlinear mixed-effects modeling techniques. The proposed model under this framework is:

$$\frac{r_{ij}^2}{R_i^2} = \left(\frac{l_{ij}}{L_i}\right)^{\beta_i} + \varepsilon_{ij} \qquad 0 \le l_{ij} \le L_i \quad (13)$$

where r_{ij} represents the j*th* ($j = 1, \ldots, n_i$) radius measurement at a length l_{ij} for the i*th* knot ($i = 1, \ldots, n$). The within-individual errors were assumed homoscedastic, normally distributed, and uncorrelated random variables with mean 0 and variance σ^2. In a preliminary analysis, the between-individual variation was accounted for by the use of a mixed-effects parameter:

$$\beta_i = \beta + b_i \quad (14)$$

where β and b_i are the fixed- and random-effects parameters, respectively. Subsequently, the estimated random-effect parameters (b_i) were re-

lated to other knot variables to incorporate covariates to explain additional between-individual variation in shape (Pinheiro and Bates 1998). Alternative model formulations were compared using twice the negative log-likelihood [$-2\ln(L)$] and the Akaike's Information Criterion (*AIC*) defined as:

$$AIC = -2\ln(L) + 2k \tag{15}$$

where L = likelihood function and k = number of parameters. The model with the smallest values for the goodness-of-fit criteria was considered the best.

The parameter estimates were evaluated by double cross-validation; the 218 branch profiles were randomly and equally split into model building and validation data set. Then, the parameters were re-estimated in the validation data set, and their stability was compared with the parameters obtained from the model-building data set. Using similar procedures for each data set, measures of precision and bias were computed and compared. The error statistics used corresponded to the mean absolute error (precision):

$$|E| = \frac{\sum_{i=1}^{n} |y_i - \hat{y}_i|}{n} \tag{16}$$

and mean error (bias):

$$E = \frac{\sum_{i=1}^{n} (y_i - \hat{y}_i)}{n} \tag{17}$$

where y_i is the observed value, $\hat{y}_i$ is the predicted value, and n is the total number of observations. After evaluation of prediction error, both data sets were combined and a final set of parameters was estimated using the entire data set making use of all available information (Myers 1990).

RESULTS AND DISCUSSION

Testing for Knot Curvature

One of the most important assumptions of the proposed model is that the internal branch inclination of knots can be assumed constant. This assumption was evaluated by fitting a separate quadratic equation to the branch pith for each knot profile considering only the live portion (see Fig 2c):

$$y_i = \beta_0 + \beta_1 x_i + \beta_2 x_i^2 + \varepsilon_i \tag{18}$$

and testing for the significance of the parameter β_2 (H_0: $\beta_2 = 0$ vs H_1: $\beta_2 \neq 0$). The test statistics was:

$$t^* = \frac{b_2}{s\sqrt{c_{jj}}} \tag{19}$$

where b_2 is the estimated parameter, s is the estimated error variance, and c_{jj} is the j*th* diagonal element of $(X'X)^{-1}$ for the quadratic model (Myers 1990). The null hypothesis was rejected if $|t^*| > t_{(1-\alpha/2),(n-3)}$. For a significance level (α) of 0.01, the null hypothesis H_0: $\beta_2 = 0$ was accepted for 192 of the 218 branch profiles. Even for those cases for which the parameter β_2 was significant, the curvature of the live portion of the knot was not severe. Based on this evidence, the inclination of knots inside the stem was assumed to be constant and a linear regression was considered appropriate to smooth the knot data.

Knot Profile Model

The fit of the model for both the model-building and validation data sets showed that parameter estimates were not different. However, in both cases, the random-effects parameter was positively related to the maximum branch radius (Fig 5). Thus, the original model was modified to represent the effect of maximum branch diameter on the shape parameter β_i. The vector of nonlinear mixed-effects parameters was modeled assuming the following form:

$$\beta_{1i} = \beta_0 R^{\beta_1 + \beta_{1i}} \tag{20}$$

where β_0 and β_1 are fixed-effects and b_{1i} is a random-effects parameter, respectively. According to the fit statistics, this model fit better for only the validation data set. However, the structure of this model was maintained because the

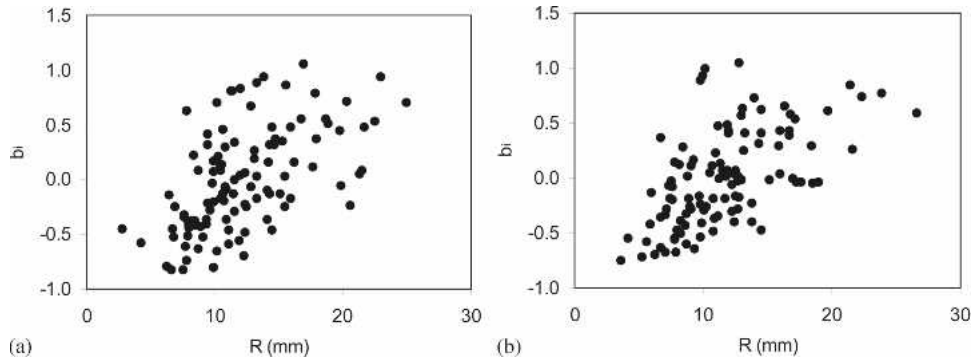

Figure 5. Relationship between the random effect parameter b_i and the maximum branch radius R_i for the (a) fitting and (b) validation data sets.

relative knot profiles appear to be clearly related to the maximum branch radius (R_i).

The validation of the model showed different behavior for both data sets. Comparatively, a larger bias was observed for the building data set using the parameter estimates obtained using the validation data set. The bias in percentage was close to 1% tending to overestimate observed values. In terms of precision, both data sets presented similar values.

A final set of parameters for the proposed model was obtained by combining both data sets (Table 1). All parameter estimates were significant and a graphical analysis showed that the model represented adequately the mean trend of observed knot profiles (Fig 6). Modeled knot profiles with smaller maximum branch diameters (R) tend to be more cylindrical than those with larger branch diameters, which presented a more parabolic or conical shape.

Model Implementation

The presented model permits modeling of different knot shapes while maintaining spatial information on internal location of live and dead portion of knots. As an example of application, let us consider that both the spatial location of knots as well as their dimensions within a whorl are required. The branch whorl is located at a stem height of 11 m on a simulated tree that has a DBH of 18 cm and a total tree height of 22 m.

This numerical example considers that the whorl contains three different types of branches, namely a live branch, a nonoccluded dead branch, and an occluded dead branch (Table 2). Both dead branches were assumed to die at the same age; however, one of them is occluded (Branch C).

The location of branches in a 3-D space can be recovered using a taper equation (Table 3). The upper stem diameters for Branch A were ob-

Table 1. *Parameter estimate and goodness-of-fit for the entire data set.*

	Estimate	SE	T	Pr > |T|
Parameter				
β_0	0.03777	0.00951	3.97	<0.0001
β_1	1.17380	0.10730	10.94	<0.0001
Variance components				
σ^2_ε	0.00158	0.00007	22.52	<0.0001
$\sigma^2_{b_1}$	0.06733	0.00747	9.01	<0.0001
Goodness-of-fit				
−2LL	−3702			
Akaike's Information Criterion	−3694			

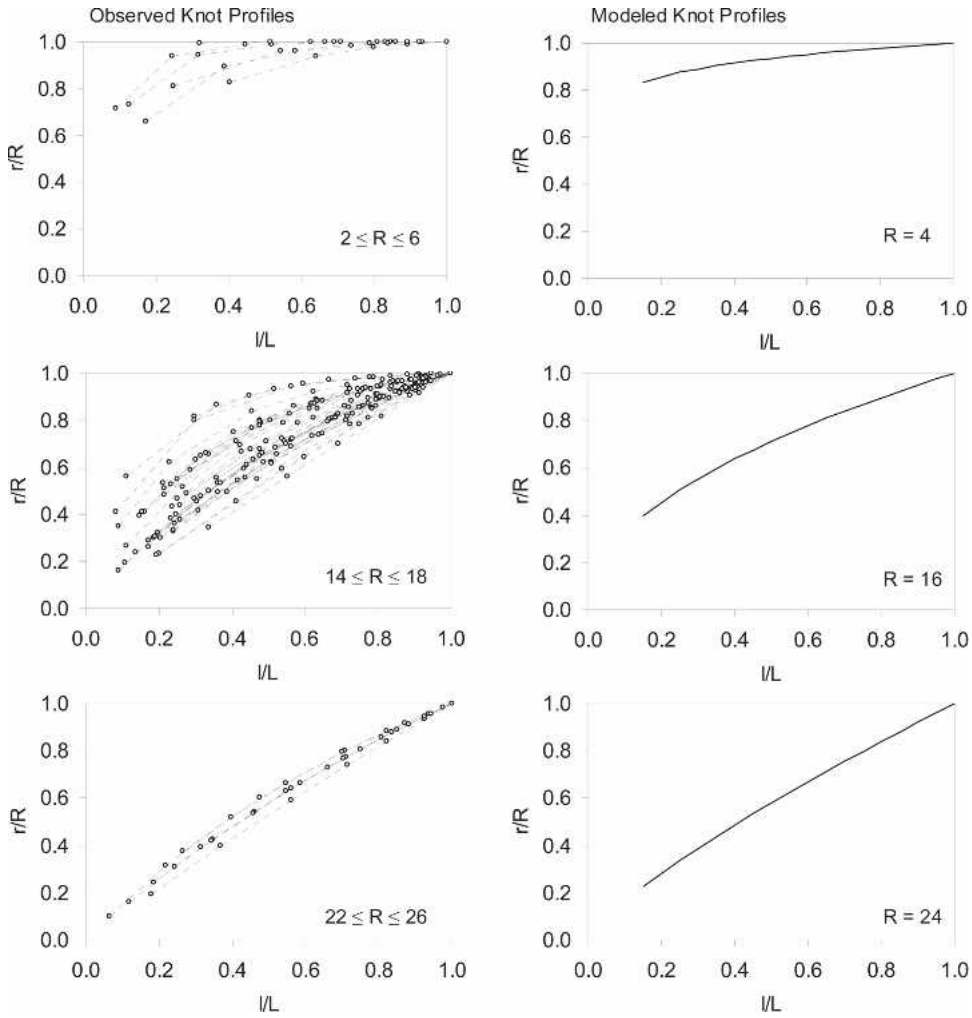

Figure 6. Observed and modeled relative knot profiles for different values of maximum branch radius (R) in millimeters.

Table 2. *Branch characteristics for a simulated whorl composed of three branches.*

Branch[a]	Type	Azimuth, θ (degrees)	Inclination, α (degrees)	Branch diameter[b] (mm)	Stem radius (cm)	
					r	r'
A	Live	45	45	35	—	—
B	Nonoccluded	285	60	20	2.8	—
C	Occluded	190	80	15	2.8	4.0

[a] See Fig 4 for additional details on the definition of each variable.
[b] Maximum branch diameter located in the live portion of a knot.

tained using the Max and Burkhart (1976) taper equation considering the following parameter values: $b_1 = -3.0257$, $b_2 = 1.4586$, $b_3 = -1.4464$, $b_4 = 39.1081$, $a_1 = 0.7431$, and $a_2 = 0.1125$. The estimated stem diameter inside bark at a stem height of 11 m is 10.39 cm.

Information on spatial location and angle of insertion of each knot is used to compute the necessary variables for estimating the volume of each knot (Table 4). The value of the shape parameter β_i is computed for each branch using Eq 20 and parameter estimates given in Table 1.

Table 3. *Spatial location of simulated branches.*

Branch	Origin (cm)			Live portion (cm)			Dead portion (cm)		
	X_O	Y_O	Z_O	X_M	Y_M	Z_M	$X_{M'}$	$Y_{M'}$	$Z_{M'}$
A	0.0	0.0	1100	3.67	3.67	1105.20	—	—	—
B	0.0	0.0	1100	−2.70	0.72	1101.62	−5.02	1.35	1203.00
C	0.0	0.0	1100	−0.49	−2.76	1100.49	−0.69	−3.94	1100.71

Table 4. *Variables required for computing knot volume.*[a]

Branch[b]	$\lvert\overrightarrow{OM}\rvert$	$\lvert\overrightarrow{MQ}\rvert$	L	l	$\lvert\overrightarrow{OM'}\rvert$	$\lvert\overrightarrow{MQ'}\rvert$	L'	l'
A	7.35	1.75	**9.10**	**3.50**	—	—	—	—
B	3.23	1.62	**4.85**	1.44	6.00	0.72	**1.87**	**1.44**
C	2.84	0.49	**3.34**	0.26	4.06	0.71	**1.43**	0.26

[a] All values are in centimeters.
[b] Values to compute volume are in bold.

Finally, the volume of the live and dead portions can be easily calculated using formulas given previously for each branch type (Table 5).

CONCLUSIONS

The procedure selected for dissecting branches allowed for recovering information on knot shape in an R/T plane. However, to get consistent information on branch growth (eg monotonically increasing branch diameter), a smoothing process was required. The equation used to smooth the data corresponded to a modified Weibull function, in which an adequate fitting was obtained when at least five observations per knot were available. In total, 15 knot samples (6.4%) failed to converge when fitting the Weibull function. A simple linear regression model was adequate to smooth branch inclination. Most of the dissected branches exhibited little or no pronounced curvature. The procedure used to smooth the raw data and reconstruct the branch profiles helped to enhance the pattern and avoid noise resulting from possible measurement errors. Recovering information on branch growth by using information of past crown recession and measurements of ring width of a disk taken above the whorl was shown to be feasible. However, no evaluation or comparison with other dissection techniques was performed. Further comparative studies on dissection techniques that evaluate accuracy, time, and operational implementation may be helpful.

Table 5. *Computed knot volumes for the live and dead portions for the simulated branches.*

Branch	Type	β_i	Volume (cm^3)		
			Live portion (LP)	Dead portion (DP)	Total
A	Live	1.09	28.59	—	28.59
B	Nonoccluded	0.73	13.74	5.65	19.39
C	Occluded	0.40	4.21	2.53	6.74

The knot model developed can represent a variety of shapes, and it allows users to readily derive analytical formulas for volume calculations. The diameter of the branches was related to their shape. Branches presenting smaller diameters were more cylindrical. Those with larger diameters were more parabolic or conical.

The use of a taper equation and additional information on angle of insertion (inclination) and horizontal orientation (azimuth) of branches allowed specification of knot spatial locations inside the stem. A numerical example showed the required steps for implementing the proposed knot model in an individual tree growth simulation system.

ACKNOWLEDGMENTS

This research was conducted at Virginia Polytechnic Institute and State University (Virginia Tech) as part of the PhD program of Guillermo Trincado. Financial support was provided through the Loblolly Pine Growth and Yield Research Cooperative at Virginia Tech, the Sustainable Engineered Materials Institute, Virginia Tech, and USDA/CSREES Fund Number 2005-06172. Necessary equipment and facilities to analyze wood samples were provided by Virginia Tech's Harvesting Research Laboratory. Drs. Philip Radtke, Carolyn Copenhaver, and

Rien Visser provided helpful advice during the development of this study. We also thank Mr. Tal Roberts and Mr. Noah Adams for valuable assistance during the dissection of whorl samples.

REFERENCES

Amateis RL, Radtke PJ, Hansen GD (2004) The effect of spacing rectangularity on stem quality in loblolly pine plantations. Can J For Res 34:498–501.

Baldwin VC Jr, Peterson KD, Clark A III, Ferguson RB, Strub MR, Bower DR (2000) The effects of spacing and thinning on stand and tree characteristics of 38-year-old loblolly pine. For Ecol Mgmt 137:91–102.

Barbour RJ, Parry DL, Punches J, Forsman J, Ross R (2003) AUTOSAW simulations of lumber recovery for small-diameter Douglas-fir and ponderosa pine from Southwestern Oregon. Res Note PNW-RN-333. USDA Forest Serv, Portland, OR.

Briggs D (1996) Modeling crown development and wood quality. J Forestry 94(12):24–25.

Clark A III, McAlister RH (1998) Visual tree grading systems for estimating lumber yields in young and mature southern pine. Forest Prod J 48(10):59–67.

———, Saucier JR, Baldwin VC, Bower DR (1994) Effect of initial spacing and thinning on lumber grade, yield, and strength of loblolly pine. Forest Prod J 44(11–12):14–20.

———, Strub M, Anderson LR, Lloyd HG, Daniels RF, Scarborough JH (2004) Impact of early pruning and thinning on lumber grade yield from loblolly pine. Pages 199–204 *in* KF Conner, ed. Proc 12th Biennial Southern Silvicultural Research Conference. Gen Tech Rep SRS-71. USDA Forest Serv, Asheville, NC.

García O (1987) A visual sawing simulator. Part II: The SEESAW computer program. Pages 107–116 *in* J A Kininmonth, ed. Proc Conversion Planning Conference. FRI Bulletin No. 128 Ministry of Forestry.

Gartner BL (2005) Assessing wood characteristics and wood quality in intensively managed plantations. J Forestry 103(2):75–77.

Grace JC, Pont D, Goulding CJ (1999) Modelling branch development for forest management. NZ For Sci 29:391–408.

Haygreen JG, Bowyer JL (1996) Forest products and wood science: An introduction. Third Edition. Iowa State University Press, Ames, Iowa. 484 pp.

Husch B, Beers TW, Kershaw JA Jr. (2003) Forest mensuration. 4th ed. John Wiley and Sons, Inc., Hoboken, NJ. 443 pp.

Judge GG, Griffiths WE, Hill RC, Lütkepohl H, Lee TC (1985) The theory and practice of econometrics. 2nd ed. Wiley and Sons, New York, NY. 1019 pp.

Kozak A (1988) A variable-exponent taper equation. Can J For Res 18:1363–1368.

Leban JM, Duchanois G (1990) SIMQUA: un logiciel de simulation de la qualité des bois. Ann Sci 47:483–493.

Lemieux H, Beaudoin M, Zhang SY (2001) Characterization and modeling of knots in black spruce (*Picea mariana*) logs. Wood Fiber Sci 33:465–475.

———, Samson M, Usenius A (1997) Shape and distribution of knots in a sample of *Picea abies* logs. Scand J Fr Res 12:50–56.

Lin C, Morse PM (1975) A compact design for spacing experiments. Biometrics 31:661–671.

Max TA, Burkhart HE (1976) Segmented polynomial regression applied to taper equations. Forest Sci 22:283–289.

Myers RH (1990) Classical and modern regression with applications. Duxbury Press, Boston, MA. 488 pp.

Neter J, Kutner MH, Nachtsheim CJ, Wasserman W (1998) Applied linear statistical models. 4th ed. McGraw-Hill Companies, Inc., Boston, MA. 1408 pp.

Pinheiro JC, Bates DM (1998) Model building for nonlinear mixed-effect models. Technical Report, Department of Statistics, University of Wisconsin–Madison. Madison, WI. 11 pp.

Samson M, Bindzi I, Kamoso LM (1996) Représentation mathématique des noeuds dans le tronc des arbres. Can J For Res 26:159–165.

Schabenberger O, Pierce FJ (2001) Contemporary statistical models for the plant and soil sciences. CRC Press LLC, Boca Raton, FL. 738 pp.

Sharma M, Burkhart HE, Amateis RL (2002) Spacing rectangularity effect on the growth of loblolly pine plantations. Can J For Res 32:1451–1459.

Todoroki CL (1996) Developments of the sawing simulation software AUTOSAW: Linking wood properties, sawing, and lumber end-use. Pages 241–247 *in* G Nepveu, ed. Second Workshop Connection between Silviculture and Wood Quality through Modelling Approaches and Simulation Softwares, Berg-en-Dal, South Africa.

West PW, Ratkowsky DA, Davis AW (1984) Problems of hypothesis testing of regressions with multiple measurements from individual sampling units. For Ecol Mgmt 7:207–224.

Whiteside ID, Wilcox MD, Tustin JR (1977) New Zealand Douglas-fir timber quality in relation to silviculture. NZ Forestry 22:24–45.

Yang RC, Kozak A, Smith JHG (1978) The potential of Weibull-type functions as flexible growth curves. Can J For Res 8:424–431.

Yu S, Chambers JL, Tang Z, Barnett JP (2003) Crown characteristics of juvenile loblolly pine 6 yr after application of thinning and fertilization. For Ecol Mgmt 180: 345–352.